ChemComm

FEATURE ARTICLE

View Article Online
View Journal | View Issue

Cite this: *Chem. Commun.*, 2022, **58**, 1871

Manipulating excited state reactivity and selectivity through hydrogen bonding – from solid state reactivity to Brønsted acid photocatalysis

Sruthy Baburaj, Lakshmy Kannadi Valloli, Jayachandran Parthiban, Dipti Garg and Jayaraman Sivaguru *

Received 30th October 2021,
Accepted 17th December 2021

DOI: 10.1039/d1cc06128c

rsc.li/chemcomm

Hydrogen bonding mediated control of photochemical reactions is highlighted with an eye towards the development of Brønsted acid mediated photocatalysis.

Introduction

The role of hydrogen bonding in evolution is quite fascinating. Recognizing these critical non-bonding interactions in biological systems, chemists have developed hydrogen bonding motifs to regulate self-assembly and control chemical reactivity.[1–4] In this feature article we will be highlighting the role of hydrogen bonding templates (Fig. 1) in controlling excited state processes both in the solid state and in isotropic media with an eye towards the development of Brønsted acid mediated photocatalysis.[2–4]

Center for Photochemical Sciences and Department of Chemistry, Bowling Green State University, Bowling Green, OH, 43404, USA. E-mail: sivagj@bgsu.edu; Web: https://www.bgsu.edu/sivagroup

Hydrogen bonding templates to control photochemical reactivity in the solid state

One of the seminal works in the area of hydrogen bonding templates mediating photochemical transformations in the solid state[5–9] was reported by Toda, Tanaka and co-workers.[10–17] Diols such as diyne-diols **Diol-1a** and **Diol-1b** (Scheme 1A and B) as well as chiral **Diol-2** derived from tartaric acid (Scheme 1C) were employed to pre-organize olefins (*e.g.* chalcones and coumarins) towards photodimerization in the solid state.[10,11] For example, photoirradiation of a powdered complex of chalcone **1** with the diacetylene diol host **Diol-1** resulted in the formation of a *syn*–head–tail (HT) dimer as the major product with >80% yield (Scheme 1A). Employing a chiral **Diol-2** for photodimerization of coumarin **5a** and thiocoumarin **5b** led to the corresponding enantioenriched

Sruthy Baburaj

Ms Sruthy Baburaj received her BS-MS in Chemistry from Indian Institute of Science Education and Research, Kolkata, India (2018). She joined the group of Prof. Jayaraman Sivaguru at BGSU in 2018 and is working towards her doctoral degree. Her research focuses on developing novel excited state phototransformations, light responsive materials and strategies to understand photodegradation in materials.

Lakshmy Kannadi Valloli

Ms Lakshmy Kannadi Valloli received her BS-MS in Chemistry from Indian Institute of Science Education and Research, Thiruvananthapuram, India (2018). She joined the group of Prof. Jayaraman Sivaguru at BGSU in 2018 and is working towards her doctoral degree. Her research focuses on developing new and novel excited state photochemical transformations and evaluation of the photophysical characteristics of compounds to understand their chemical reactivity.

photoproducts with excellent yield and high optical purity (~100% ee) in the solid state (Scheme 1C).

Nakamura and co-workers[18] utilized the coumarin motif as part of the hydrogen bonding template that was derived from Kemp triacid (**KTT1**). The **KTT1** template served both as a light-absorbing motif and as an anchoring unit to facilitate photocycloaddition with thymine **7**. The hydrogen bonding interaction coupled with facial differentiation during photoreaction led to the exclusive formation of *cis–syn* adduct **8**. The formation of the *cis–syn* adduct was postulated to occur through a ''*cis–syn*-complex'' that featured favorable interactions due to ''ππ–stacking'' when compared to ''*cis–anti* complex''. This led to an attractive overlap of the direction and the distance of the reactive double bonds leading to the formation of *cis–syn* adduct **8** (Scheme 2). MacGillivray and co-workers employed resorcinol (1,3-dihyroxybenzene) **Diol-3** as a host template to control photochemical reactivity of molecules in the solid state.[19–21] Olefins featuring pyridyl rings (*e.g.*, **9**) were templated towards photodimerization in the solid-state (Scheme 2) leading to photoproduct **10** with excellent control of reactivity. A similar strategy was also extended to other olefins such as pyridylethylenes, dienes and trienes.[21,22] They also employed the Kemp triacid derived template **KTT2** for dimerization of **9** (Scheme 2) leading to the selective formation of photoadduct **10**.[23] While H-bonding directed reactivity in crystalline media gave insights into molecular reactivity, it was not generally applicable to compounds that were not crystalline. In addition, translating the interactions for asymmetric photoreactions for a diverse set of compounds necessitated that the strategy had to be extended to solution phase reactions with the knowledge gained from solid-state studies.

H-Bonding templates for controlling enantioselective photochemical transformations in solution

One of the recent advances made by photo chemists involve the use of hydrogen-bonding templates for controlling enantioselective photochemical transformations in isotropic media (Scheme 3). Bach and co-workers have extensively utilized Kemp triacid derived templates (**KTT3-KTT6**; *cf.* Schemes 3 and 4) to control photochemical transformations and to achieve stereoselectivity in solution.[24–27] The Kemp triacid lactam template (+)-**KTT3** or (-)-**KTT4** was utilized for controlling the enantioselective transformations of 4-substituted quinolone **11** (Scheme 3).[24] [2+2]-Photocycloaddition reactions of quinolone **11a** with Kemp triacid lactam templates (-)-**KTT4** (Scheme 3) resulted in low enantioselectivity of 37% in photoproduct **12a** with 89% yield at −15 °C in toluene. The weak association between **11** and (-)-**KTT4** when compared to (+)-**KTT3** was rationalized for the observed low and high enantioselectivity with the two hosts. The enantioselectivity increased to 93% (77% yield) when 2.6 equivalents of (+)-**KTT3** was employed at −60 °C. Photocycloaddition of

Jayachandran Parthiban

Mr Jayachandran Parthiban received his MSc in Chemistry from Madras Christian College, India (2011). He spent 2 years in Academia Sinica, Taiwan. He joined the research group of Prof. Jayaraman Sivaguru at BGSU in 2019 and is working towards his doctoral degree. His research is focused on developing new catalytic methods for photochemical transformations and developing new materials for optical applications and eye protection as well as understanding the excited state phenomenon using photophysical methods.

Dipti Garg

Ms Dipti Garg received her MSc in Chemistry from Indian Institute of technology, Madras (IIT-M), Chennai, India (2019). She spent 1 year as a junior researcher in the Research & Development Centre, Dabur, India. She joined the group of Prof. Jayaraman Sivaguru at BGSU in 2020 and is working towards her doctoral degree. Her research focuses on exploring excited state reactivity for developing novel photocycloaddition reactions. She is also involved in the design, synthesis and evaluation of next-generation optical materials for eye protection.

Jayaraman Sivaguru

Prof. Dr Jayaraman Sivaguru (Siva) is the Antonia and Marshall Wilson Professor of Chemistry and the Associate Director for the Center for Photochemical Sciences at the Department of Chemistry, Bowling Green State University, Bowling Green, Ohio. Prof. Sivaguru is well known for his contributions to the area of photochemical sciences. He has been recognized with numerous awards over the last decade. In 2021, Prof. Sivaguru was the recipient of the Honda–Fujishima Lectureship award from the Japanese photochemical association. His research program includes studies from both the fundamental and applied aspects of photochemistry.

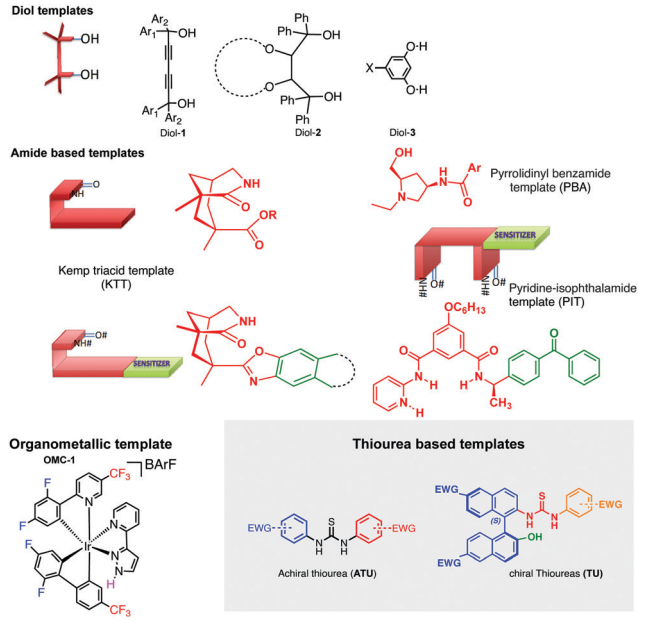

Fig. 1 Hydrogen bonding templates for controlling excited state transformations.

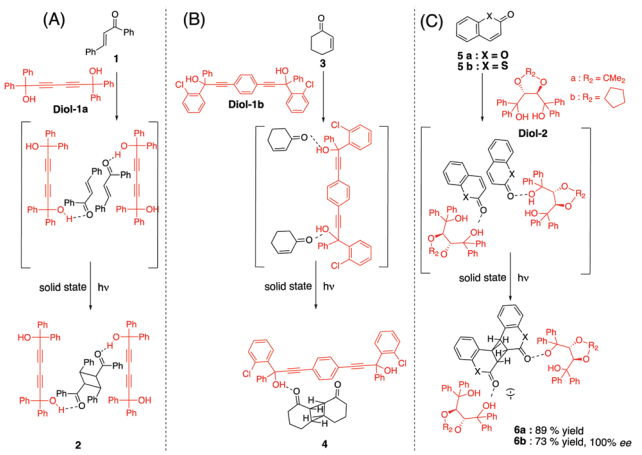

Scheme 1 Hydrogen bonding diols as crystalline hosts for photochemical transformations in the solid state.

quinolone **11c** featuring a longer alkyl chain with 1.2 equivalents of chiral host (+)-**KTT3** in toluene at −15 °C resulted in 88% enantioselectivity with 88% yield. In spite of not being sub-stochiometric, the study clearly provided guidelines for employing hydrogen bonding templates for enantioselective transformations in isotropic media.

Inoue and co-workers[28] utilized a pyrrolidinyl benzamide (**PBA**) derived chiral H-bonding template (Scheme 3) for controlling enantioselective photodimerization of anthracenecarboxylic acid **14**. Photodimerization of **14** was evaluated in the presence of the **PBA** template in dichloromethane at two different temperatures (25 °C and −50 °C). The **PBA1** template featuring a *cis* geometry between the amide and alcohol functionality gave 25–43% enantioselectivity in the *syn*-HT-**15**

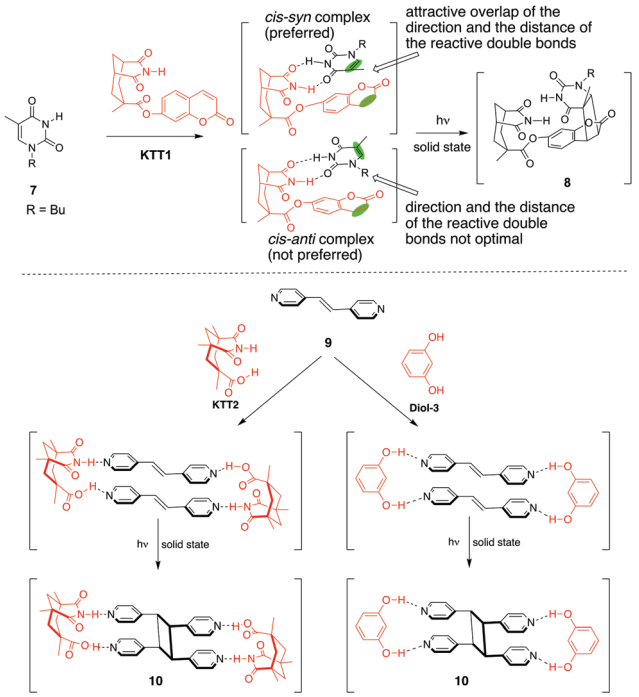

Scheme 2 Dimerization of dienes and trienes templated using hydrogen bonding hosts.

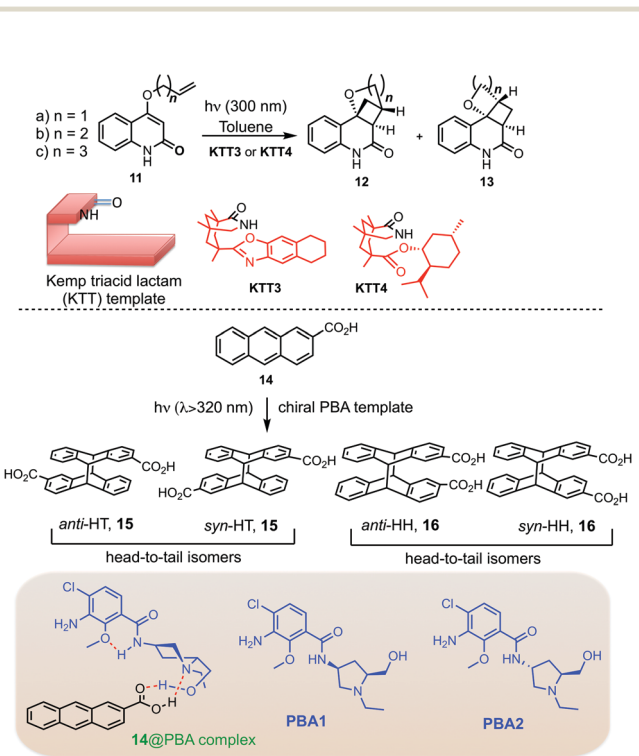

Scheme 3 Hydrogen bonding templates for controlling stereoselective phototransformations in solution.

photoproduct and 10–43% enantioselectivity in the *anti*-HT-**15** photoproduct. A low enantiomeric excess (<3% ee) of photoproducts was observed when the **PBA2** template featured a *trans* geometry between the amide and alcohol functionality. Based

on the single crystal XRD analysis of the **14@PBA** complex, the authors reasoned that the interaction of the **PBA** template with **14** in the hydrogen-bonded complex led to a preferential attack from the open enantioface of **14** bound to the chiral template. Thus, the study clearly established that the geometric features (*cis*/*trans* relation) in **PBA1** and **PBA2** were crucial in the stereodifferentiation processes.

Sensitizing H-bonding templates for enantioselective phototransformations

The hydrogen bonding template also served as a sensitizing unit enabling energy transfer or electron transfer.[25–27] Appending a hydrogen bonding template to a sensitizer provides an avenue to bring the reactive substrate(s) in close proximity, enabling energy or electron transfer leading to efficient photochemical reactivity coupled with stereodifferentiation.

Krische and co-workers[29] utilized a benzophenone triplet sensitizer that was appended to a chiral pyridine-isophthalamide template (**PIT**) for performing enantioselective [2+2]-photocycloaddition of quinolones **11b** (Scheme 4). Hydrogen bond enabled host–guest complex formation between the template and the substrate was rationalized for the enhanced photoreactivity of **11b** in the presence of 0.25–2 equivalents of the **PIT** template in $CDCl_3$ at −70 °C. The reaction mechanism was postulated to occur through triplet energy transfer from benzophenone to the substrate that led to enhanced photoreactivity. In spite of the increased photoreactivity, a low enantiomeric excess of ∼20% was observed in photoproduct **12b** (Scheme 4).

Bach and co-workers[25–27] utilized chiral sensitizers appended to a Kemp lactam host for both electron and energy transfer mediated phototransformations (Scheme 4).[25–27] They employed the xanthone appended Kemp lactam host **KTT5** for photoinduced electron transfer reaction with quinolone **17** (Scheme 4) leading to 70% enantioselectivity with 64% yield of photoproduct **18**. The mechanism involved a photo-induced electron transfer followed by a proton transfer leading to the formation of diradical intermediate(s), that cyclized to form **18**.

Bach and co-workers[25–27] also extended the strategy for energy transfer initiated intramolecular [2+2]-photocycloaddition of quinolone **11b**. With the benzophenone appended host **KTT6** (10 mol%), low enantioselectivity of 39% was observed in photoproduct **13b** at −25 °C. On the other hand, the xanthone appended host **KTT5** (5 mol%) gave a high enantioselectivity of 90% in photoproduct **13b**. The regioisomeric ratio was 79 : 21 for photoproducts **12b** : **13b**. In both the cases, the reaction mechanism involved triplet energy transfer leading to diradical intermediates *en route* to the formation of the photoproduct. The absorptivity and low triplet energy of benzophenone when compared to xanthone was highlighted to be a crucial factor for the observed difference in stereoselectivity between the two templates.

Organometallic complexes as hydrogen bonding templates for photoreactions

Based on the report by Meggers and co-workers[30] on employing iridium(III) photocatalysts bearing electron-deficient cyclometalated phenyl pyridine, Yoon and co-workers[31] employed ligands featuring Brønsted acidic sites for hydrogen-bonding asymmetric photocatalysis. They revealed the intramolecular photocycloaddition of 3-alkoxyquinolone **19** that showed a low triplet energy that was amenable to energy transfer from the iridium based organometallic catalyst **OMC-1a** at 1 mol% loading with blue LEDs at −70 °C leading to photoproduct **20** in 98% yield with an enantioselectivity of 49% (Scheme 5). Both the thiomethyl-substituted catalyst **OMC-1e** and the unsubstituted catalyst **OMC-1f** gave 69% enantioselectivity in the product **20**.

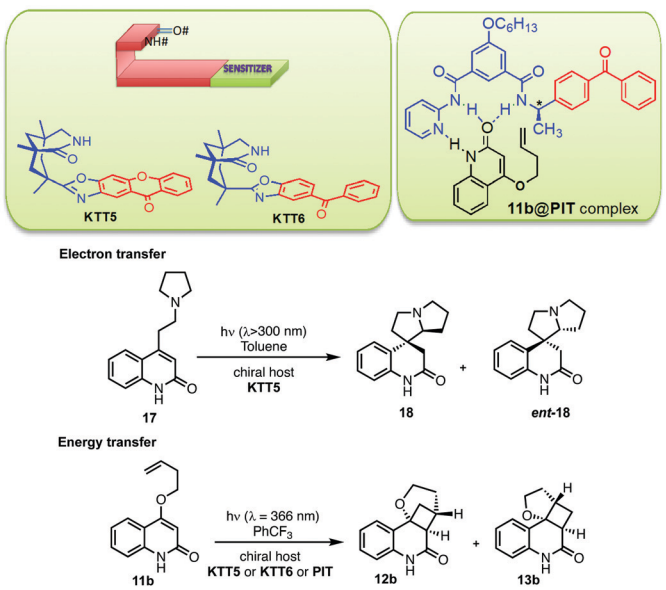

Scheme 4 Sensitizing hydrogen bonding templates for controlling electron transfer and energy transfer mediated enantioselective phototransformations.

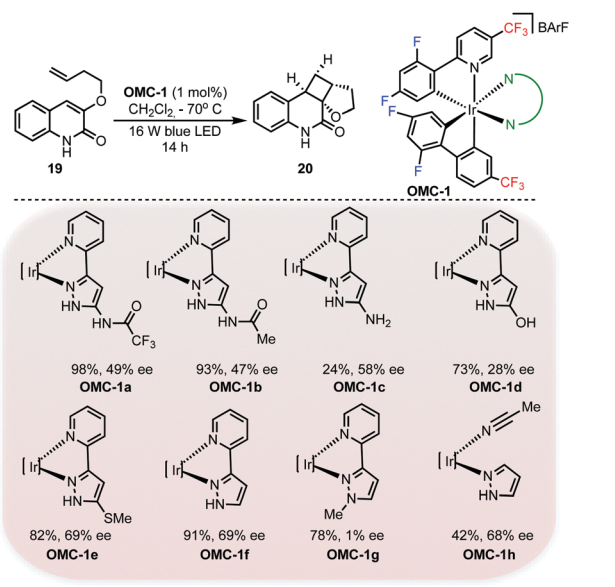

Scheme 5 Organometallic hydrogen bonding motifs for enantioselective [2+2]-photocycloaddition.

Phosphoric acid based hydrogen bonding templates for organo-photocatalysis

Bach and co-workers utilized chiral phosphoric acid template **PAT-1** to evaluate asymmetric inter-molecular [2+2] photocycloaddition of cyclic enones **21** (Scheme 6) with different alkenes **22a–c**.[32] This **PAT-1** template featured two thioxanthone moieties connected to a 2,2′-binapthol system at the 3,3′ position. Photoirradiation of enone **21** and alkene **22a–c** in the presence of the **PAT-1** catalyst led to the corresponding cyclo-adducts **23a–c** with reasonable yields (30–40%) and good enantioselectivity (70–80% ee). Bach and co-workers also explored the mechanism by NMR studies and DFT calculations and proposed that the enantioface differentiation through triplet energy transfer that was promoted by hydrogen bonding mediated interactions between the **PAT-1** photocatalyst and enones **21** (Scheme 6).

Thiourea based hydrogen bonding templates for organo-photocatalysis

While the hydrogen bonding templates reviewed above were very effective for enantioselective phototransformations, a systematic investigation for manipulating the stereo-electronic features of the organo-photocatalyst (similar to ground state reactions) for asymmetric phototransformation was lacking. It became critical to perform an in-depth study of photophysical and photochemical features and how the energetics and dynamics in the excited state impacts the design of novel organo-photocatalysts for excited state transformations.[33–35] This is because the nature of the excited state might be altered when the stereo-electronic features of the catalysts are altered by varying the substituents.[36] To overcome this, research from our group[33–35] has showcased the use of thioureas as a template are amenable to systematic stereo-electronic variations to achieve high asymmetric induction during excited state transformations.

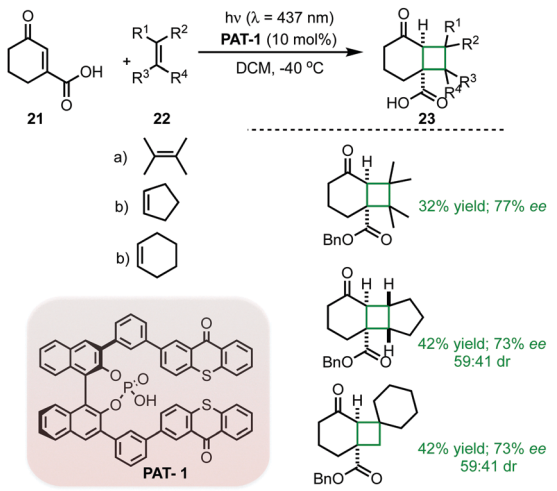

Scheme 6 Chiral phosphoric acid as an organophotocatalyst for inter-molecular [2+2] cycloaddition.

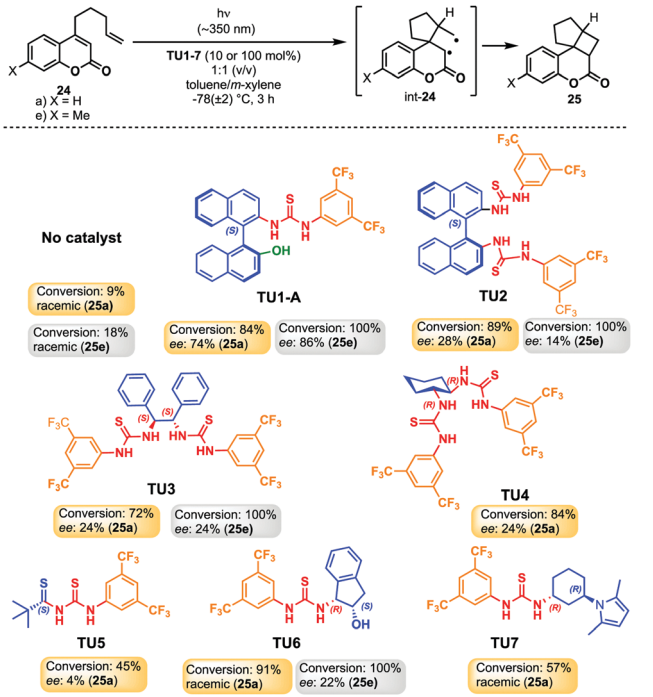

Scheme 7 Thiourea based hydrogen bonding motifs for enantioselective [2+2]-photocycloaddition.

To perform a systematic evaluation of organo-photocatalyst substrate interactions and its impact on excited state reactivity, intramolecular [2+2]-photocycloaddition of 4-alkenylcoumarin **24** was evaluated with thiourea catalysts **TU1-7** leading to photoproduct **25** (Scheme 7).[34] The reason we selected thioureas as templates for evaluating photoreactions is due to the myriads of advantages they provide over other systems *viz.*, (a) they are easy to synthesize often in a few steps; (b) the catalysts do not require any special handling and are stable in moisture and in aerated atmospheres; (c) thioureas can be easily fine-tuned to influence their hydrogen bonding ability with electron-donating and/or electron withdrawing groups. More importantly, altering the nature of the thiourea catalysts with various substituents will not only provide us with a systematic overview of how the catalyst interacts with substrates, but also how the excited state chemistry is influenced *i.e.*, both dynamics and energetics of excited state and its impact on the photochemical reactivity of the system under investigation can be evaluated.

Chiral thiourea catalysts that have been successful for thermal asymmetric reactions were evaluated for intramolecular [2+2]-photocycloaddition of alkenyl-coumarin **24a** leading to the corresponding cyclized photoproduct **25a** (Scheme 7). The monofunctional Ricci's catalyst **TU6** and **TU7** gave excellent conversions of 91% and 57%, respectively, when compared to 9% conversions for non-catalysed reaction under similar conditions (1 : 1 toluene/*m*-xylene at −78 °C for 3 h). Despite the high conversions, the observed photoproduct **25a** was a racemic mixture. Based on NMR titration experiments, the interaction between the coumarin substrate and the catalyst

was established. The binding constant for **24e-TU6** interaction was ascertained to be 14.8 (±1.2) M^{-1} in $CDCl_3$. Monofunctional thiourea **TU5** gave 45% conversion with 4% ee in photoproduct **25a.** The C_2-symmetrical bis-thiourea catalyst **TU3** and **TU4** gave a conversion of 72% and 84% respectively with a moderate enantiomeric excess of 24% in photoproduct **25a.** The atropoisomeric bis-thiourea catalyst **TU2** gave a conversion of 89% with 28% enantiomeric excess in **25a.** As the atropoisomeric systems gave moderate enantioselectivity, the NOBIN-derived thiourea catalyst **TU1** was employed for the intramolecular [2+2]-photocycloaddition of **24a** that led to 84% conversions with 74% ee in the corresponding photoproduct.

As the NOBIN-derived thiourea catalyst **TU1-A** showed promising reactivity towards enantioselective intramolecular [2+2]-photocycloaddition of **24a**, the electronic features of the thiourea catalyst were further manipulated to understand the origin of enhanced photoreactivity and the stereodifferentiation mechanism (Scheme 8).[33] Enantioselective intramolecular [2+2]-photocycloaddition of **24a** with **TU1-A** was kept as a reference for evaluating other NOBIN-derived thiourea catalysts as it gave 84% conversion and 74% ee in 1 : 1 toluene/*m*-xylene at −78 °C. To understand the role of the hydrogen bonding motif, the thiourea functionality in **TU1-A** was changed to a urea functionality in **TU1-B.** Intramolecular [2+2]-photocycloaddition of **24a** with **TU1-B** gave 46% conversion with 28% enantioselectivity. The precipitous drop in both conversion and enantioselectivity showed the importance of the thiourea functionality facilitating the enantioselective transformation. To understand the role of substituents on the *N*-phenyl ring on the thiourea, the 3,5-trifluoromethyl substituents in **TU1-A** was changed to the tetrafluoro-substituted phenyl ring in **TU1-C** that resulted in a minimal change in the enantioselectivity (74% ee in **TU1-A** and 71% ee in **TU1-C**) and conversions (84% for **TU1-A** and 85% for **TU1-C**). To probe the role of binaphthyl-substituents and their impact on the hydrogen-bonding ability, the hydroxyl substituent on the naphthyl ring was systematically varied (compare **TU1-A** and **TU1-D**/**TU1-E**). Replacing the hydroxyl substituent in **TU1-A** with the methoxy substituent in **TU1-D** resulted in a low conversion of 9% (from 84% in **TU1-A**) with 11% enantioselectivity (from 74% ee with **TU1-A**). A point to note was that the optical antipode *ent*-**24a** was observed in excess with **TU1-D** when compared to **TU1-A.** Employing **TU1-E** as the catalyst that lacked the hydroxyl substituent on the binaphthyl ring resulted in a conversion of 50% with low enantioselectivity of 7% in the photoproduct. Having ascertained the importance of the hydrogen bonding unit appended to the bi-naphthyl ring, thioureas **TU1-F** and **TU1-G** that featured electron withdrawing CF_3 groups at the 6- and 6′-positions of the binaphthyl backbone were evaluated. Intramolecular [2+2]-photocycloaddition of **24a** with **TU1-F** led to conversions of 95% with 90% enantioselectivity in photoproduct **25a.** Similarly, thiourea **TU1-G** gave quantitative conversions with 96% enantioselectivity photoproduct **25a** (Scheme 8).

To evaluate the impact of the catalytic loading level, enantioselective [2+2]-photocycloaddition of coumarin **24a** was performed with varying amounts (1–100 mol%) of the best performing thiourea catalyst **TU1-G** (Scheme 9). Employing 10 mol% of **TU1-G** led to quantitative conversions within 30 min of irradiation with 94% enantioselectivity in photoproduct **25a.** The efficiency of asymmetric induction was also maintained in large scale reactions with 77% isolated yield and 92% enantioselectivity in the product. Decreasing the loading level of the catalyst to below 10 mol% led to a slight decrease in the enantiomeric excess which was rationalized due to the competing background reactions at low loading levels.

The generality of enantioselective photocycloaddition catalyzed by thiourea **TU1-G** (10 mol%) was evaluated with coumarin derivatives **24a–f** (Scheme 10). Varying the substituent at the 6-position of coumarin to an electronic rich methyl group

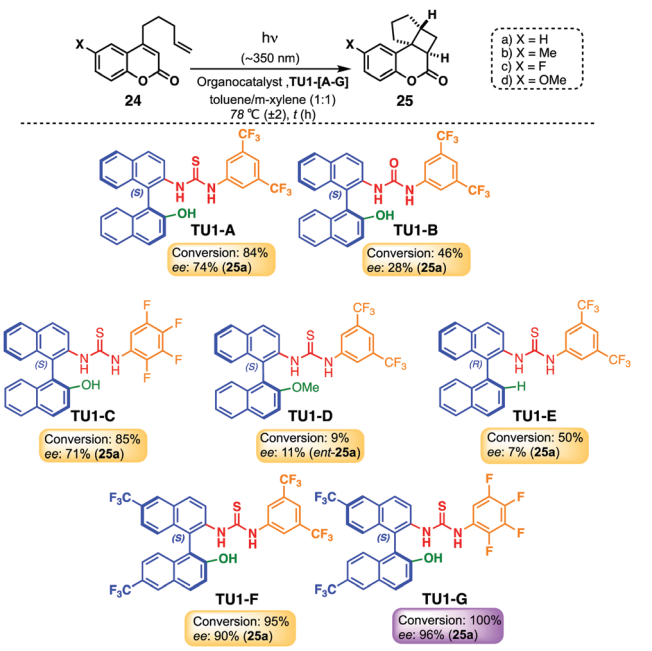

Scheme 8 Modulating the stereo-electronic features of NOBIN-derived thiourea catalyst for enantioselective [2+2]-photocycloaddition.

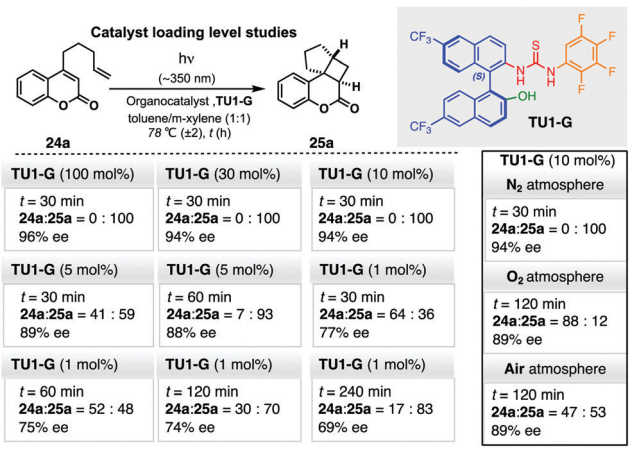

Scheme 9 Enantioselective [2+2]-photocycloaddition of coumarin **24a** with various loading levels of thiourea catalyst **TU1-G**.

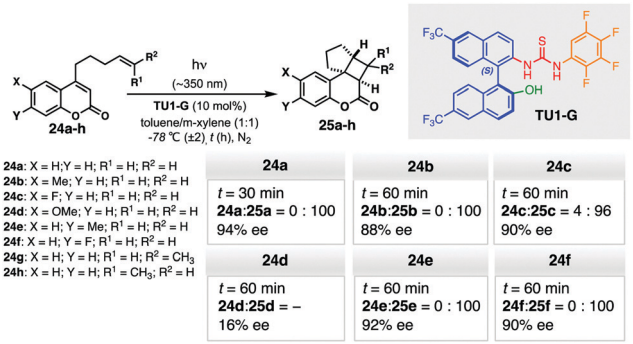

Scheme 10 Substrate scope for enantioselective [2+2]-photocycloaddition of coumarin derivatives with thiourea catalyst **TU1-G**.

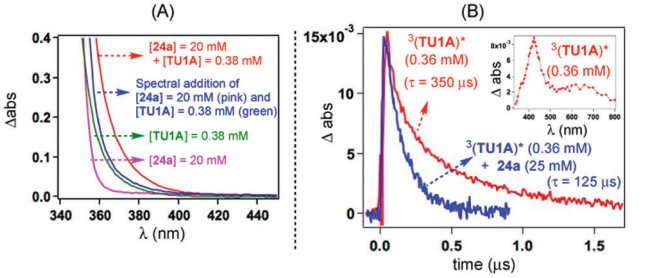

Fig. 2 Photophysical investigations for ascertaining catalyst–substrate interactions. (A) UV/Vis absorption spectra in methylcyclohexane (MCH). (B) Transient absorption decay traces of ^{3}(**TU1-A**)* monitored at 425 nm after pulsed laser excitation (355 nm, 5 ns) and transient absorption spectrum of **TU1-A** in deoxygenated MCH (inset). Reproduced with permission from ref. 33. Copyright 2014 John Wiley and Sons.

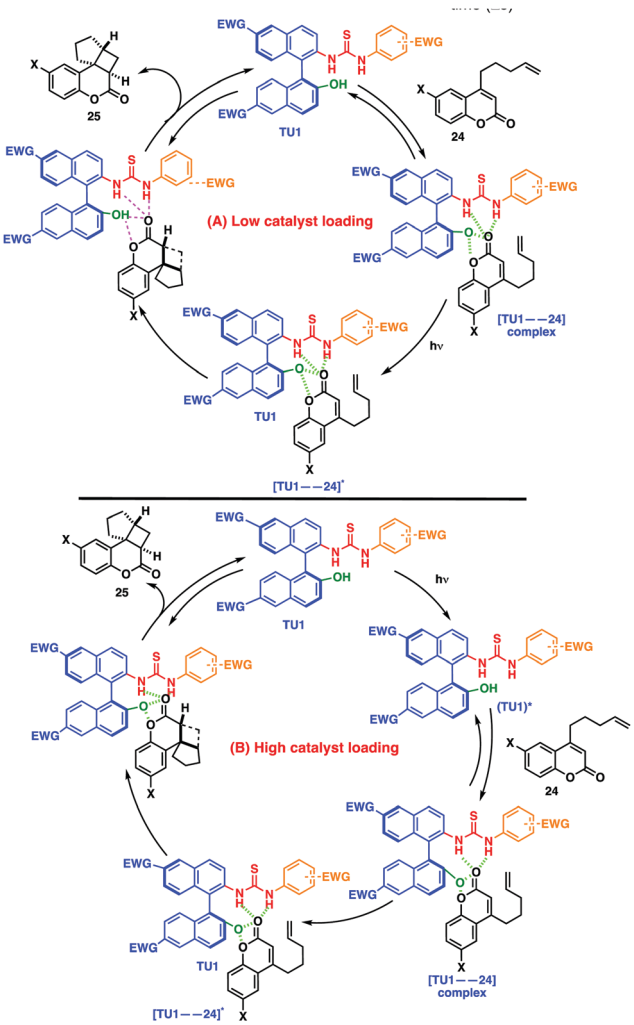

Fig. 3 Mechanistic features of thiourea mediated enantioselective organo-photocatalysis at low (top) and high (bottom) catalytic loading levels. Adapted from ref. 33. Copyright 2014 John Wiley and Sons.

(*e.g.*, **24b**) and an electron deficient fluorine substituent (*e.g.*, **24c**) resulted in 88% and 90% enantioselectivity in the corresponding photoproduct. There was a significant drop in the enantioselectivity to 16% when methoxy coumarin **24d** was employed for [2+2]-photocycloaddition. This revealed that the hydrogen-bonding interaction between the thiourea catalyst and the substrate was disturbed by the 6-methoxy substituent in **24d**. Thiourea catalyst **TU1-G** (10 mol%) was also effective for enantioselective [2+2]-photocycloaddition of 7-substituted coumarins **24e** and **24f** leading to enantioselectivity of 92% and 90%, respectively. The reaction atmosphere had a profound impact on the reaction efficiency but the enantioselectivity was not significantly affected (Scheme 9). Photoreaction of **24a** with 10 mol% of **TU1-G** under nitrogen, oxygen and aerated conditions gave quantitative, 12% and 53% conversions, respectively. In spite of the variation in conversion the enantioselectivity was not affected significantly, which showed a reactive triplet diradical intermediate int-**24** (Scheme 7). This was further confirmed by employing internal alkenes **24g** and **24h** (Scheme 10) with thioureas **TU1-A** that showed scrambling of the alkene geometry *i.e.*, *cis*/*trans* isomerization of the alkene double bond was observed in addition to the photocycloaddition reaction. These once again pointed to the involvement of a triplet 1,4-biradical int-**24** (Scheme 7) during the catalytic process.

The role of the **TU1-A** catalyst in promoting the photoreaction was investigated by performing extensive photophysical studies. The absorption spectra of the substrate shifted bathochromically (Fig. 2A) in the presence of the thiourea catalyst. Even though the excited state energy of substrate **24a** (excited singlet-state E_s = 84 kcal mol^{-1} and excited triplet-state E_T = 64 kcal mol^{-1}) was higher than that of thiourea catalyst **TU1-A** (excited singlet-state E_s = 77 kcal mol^{-1} and excited triplet-state E_T = 58 kcal mol^{-1}) the photoproduct was generated efficiently during the photoreaction. There was also efficient quenching of the **TU1-A** excited state by coumarin substrate **24a**. Transient absorption measurements showed a dynamic complex between catalyst and the reactant (Fig. 2B). This led to the suggestion of a dual catalytic cycle depending on the loading level of the catalyst and the hydrogen-bonding interactions between **TU1-A** and the coumarin substrate (Fig. 3).

The light absorbing species was likely determined by the catalyst loading level (Fig. 2A). At low catalyst loading levels, the catalyst–substrate complex had a bathochromic shift in the

absorption spectrum. This catalyst–substrate complex upon photoexcitation reacted efficiently to form the product *via* a triplet 1,4-diradical (Fig. 3-top). At high catalyst loading levels (Fig. 3-bottom), the thiourea catalyst was excited due to its higher absorptivity. The catalyst excited state was quenched effectively by the substrate in spite of the excited state energy mismatch as they proceed through an exciplex. This exciplex reacted effectively to form the photoproduct through a triplet 1,4-diradical intermediate.

Our group also extended the strategy of employing thioureas for catalysing intermolecular [2+2]-photochemical reactions of coumarin **26** with alkene **27** leading to photoproduct **28** (Scheme 11).[35] In the absence of any thiourea catalyst the reaction was inefficient with <4% conversion. However, in the presence of the achiral thiourea **ATU1-5** the conversion ranged from 22 to 76% with the naphthyl substituted achiral thiourea **ATU5** being the most effective for the intermolecular photocycloaddition (Scheme 11). The photocycloaddition reaction with 10 and 5 mol% of **ATU5** gave a reactant to product ratio (**26**:**28**) of 1:99 and 57:43, respectively (Scheme 11). The achiral thiourea **ATU4** was found to interact with both reactant **26** and photoproduct **28** with an association constant (K_a) of 6.3 M^{-1} and 4.8 M^{-1}, respectively.

Photophysical investigations revealed that there was no bathochromic shift in coumarin absorption in the presence of achiral thioureas **ATU**s (Scheme 11) which was quite different from what was observed for NOBIN-derived thioureas **TU**s (Scheme 7). There was no appreciable fluorescence from **26** in toluene at room temperature while strong fluorescence centred around 408 nm and weak phosphorescence overlapping with the fluorescence signal were observed at 77 K in methylcyclohexane (MCH) glass. Kinetic decay analysis of the luminescence at 412 nm showed two lifetimes of 1.2 ns and 4.0 ns. It was conjectured that the emission characteristics are due to the monomer and the dimeric aggregate of **26** in MCH glass at 77 K. Luminescence measurements with a 1:1 mixture of catalyst **ATU4** and **26** displayed a reduction in the coumarin

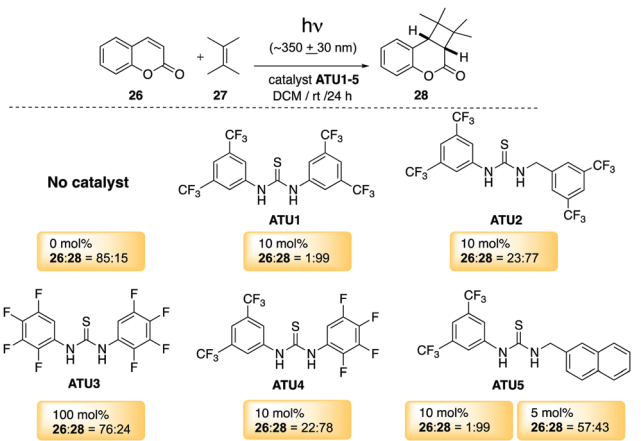

Scheme 11 Achiral thiourea (**ATU**) as an organo-photocatalyst for the intermolecular [2+2]-photochemical reaction of coumarin **26** with tetramethyl ethylene **27**.

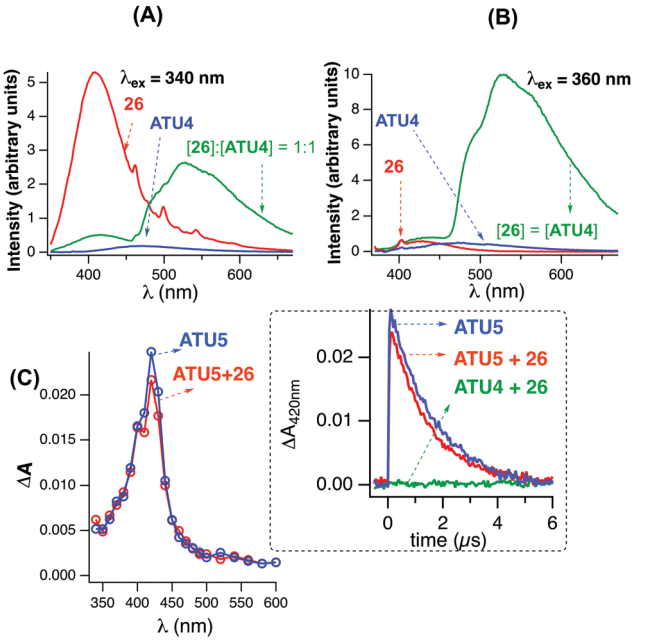

Fig. 4 Photophysical investigations for deciphering the role of achiral thioureas in promoting intermolecular [2+2]-photocycloaddition. (Top) Steady-state luminescence spectra with λ_{ex} = 340 nm (A) and λ_{ex} = 360 nm (B). (Bottom) Transient absorption spectra recorded 0–0.4 μs after pulsed laser excitation (λ_{ex} =355 nm, 5 ns pulse width) of argon-saturated toluene solutions of **ATU5** (2 mM) in the absence (blue) and presence (red) of **26** (2 mM). Inset: Absorbance kinetic traces monitored at 420 nm. Reproduced with permission from ref. 35. Copyright 2014 John Wiley and Sons.

fluorescence as well as its corresponding lifetimes at 412 nm (*i.e.*, 0.6 ns and 3.2 ns). In addition, the emission intensity of the 1:1 mixture of **ATU4** and **26** depended on the excitation wavelength (compare Fig. 4A and B). Excitation at 340 nm displayed weak emission from the coumarin and a new emission centred at approximately 523 nm was observed, while excitation at 360 nm where coumarin **26** does not have any absorption displayed predominantly the new emission band centred around 523 nm. This emission was rationalized due to the selective excitation of the coumarin–catalyst complex. The properties of the triplet states of coumarin and achiral thiourea **ATU5** were investigated by phosphorescence spectroscopy in a toluene matrix at 77 K that revealed a ππ* configuration in both the catalyst and the reactant. Pulsed laser excitation of a 1:1 mixture of **26** (2 mM) and achiral thiourea **ATU5** at 355 nm generated a transient absorption spectrum with a maximum at 420 nm (Fig. 4C, red spectrum), which decayed monoexponentially with a lifetime of 1.5 μs (Fig. 4C). A similar transient absorption spectrum was observed in the absence of **26** indicating that it originates from the excited catalyst. This transient absorption generated from **ATU5** was not quenched by coumarin **26** as well as by **27** even at a high concentration indicating the naphthalene triplet in **ATU5** was not involved in enhancing the rate of the reaction. Based on these studies a mechanistic model was proposed (Fig. 5) in which the enhanced intermolecular [2+2]-photocycloaddition of **26** in

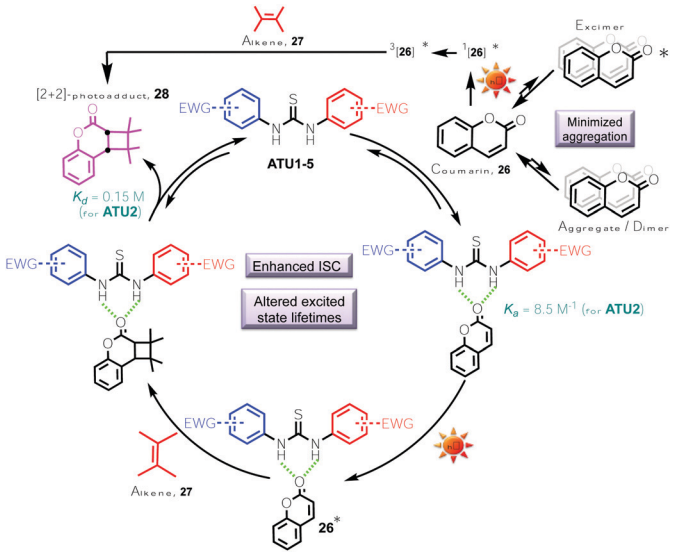

Fig. 5 Mechanistic details for the organo-photocatalytic intermolecular [2+2]-photochemical reaction of coumarin **26** with tetramethylethylene **27**. Adapted with permission from ref. 35. Copyright 2014 John Wiley and Sons.

the presence of achiral thioureas was due to the minimized aggregation of coumarin **26** (based on luminescence studies in MCH, Fig. 4A and B). In addition, the phosphorescence showed an enhanced intersystem crossing (ISC) in coumarin, that was reflected in the enhancement of the phosphorescence signal along with altered excited-state lifetimes. The change in the above excited-state properties was initiated by hydrogen bonding interaction between the reactant and the thiourea catalyst. Thus, the investigation revealed the diverse function of thiourea catalysts in both intramolecular [2+2]-photocycloaddition (Schemes 6–9) and intermolecular [2+2]-photocycloaddition (Scheme 11).

Future outlook on Brønsted acids mediated excited state asymmetric photochemical transformations

One of the critical aspects that researchers need to consider when designing organo-catalysts in general for excited state transformations is how the substitution will affect the energy and dynamics of the excited state.[33–35] This requires an in-depth study of photophysical features in addition to evaluating the photochemical aspects.[33–35] Combining the knowledge gained from both photochemical and photophysical measurements new and exciting aspects related to excited state asymmetric photochemical reactions can be evaluated in depth to enhance its utility and scope.

Conclusions

The rich chemistry of hydrogen bonding mediated photochemical transformations has certainly evolved from reactions in crystalline media to asymmetric phototransformations from solution. Since our report on utilizing thioureas as organo-photocatalysts, multiple groups have utilized thiourea derived catalysts for controlling photochemical reactions.[37,38] Recently, Brønsted acids derived from phosphoramide have shown potential in intermolecular asymmetric [2+2]-photocycloaddition reactions.[39] These developments are certain to pave a way for a bright and fruitful evaluation of Brønsted acid mediated organo-photocatalysis.[40]

Author contributions

This Feature article was written by all the co-authors under the guidance of JS.

Conflicts of interest

The authors declare no conflicts.

Acknowledgements

The authors are grateful for the generous support from NSF for their program (CHE-1955524). The authors thank their collaborators Prof. Mukund Sibi and Dr Steffen Jockusch as well as all the students and post-doctoral associates for their seminal contributions in the development of enantioselective Brønsted acid mediated organo-photocatalysis.

Notes and references

1 J.-M. Lehn, *Supramolecular Chemistry: Concepts and Perspectives*, VCH, New York, 1995.
2 N. J. Turro and M. Garcia-Garibay, in *Photochemistry in Constrained Media*, ed. V. Ramamurthy, VCH Publishers, Inc., 1991, ch. 1, pp. 1–38.
3 F. H. Quina and D. G. Whitten, *J. Am. Chem. Soc.*, 1977, **99**, 877–883.
4 *Supramolecular Photochemistry*, V. Balzani and F. Scandola, ed., Ellis Horwood, Chichester, 1991.
5 J. Bregman, K. Osaki, G. M. J. Schmidt and F. I. Sonntag, *J. Chem. Soc.*, 1964, 2021–2030.
6 G. M. J. Schmidt, *Reactivity of the Photoexcited Organic Molecule*, Interscience, New York, 1967, pp. 227–284.
7 G. M. J. Schmidt, *Pure Appl. Chem.*, 1971, **27**, 647–678.
8 K. Gnanaguru, N. Ramasubbu, K. Venkatesan and V. Ramamurthy, *J. Org. Chem.*, 1985, **50**, 2337–2346.
9 K. Muthuramu and V. Ramamurthy, *J. Org. Chem.*, 1982, **47**, 3976–3979.
10 K. Tanaka, E. Mochizuki, N. Yasui, Y. Kai, I. Miyahara, K. Hirotsu and F. Toda, *Tetrahedron*, 2000, **56**, 6853–6865.
11 K. Tanaka and F. Toda, *J. Chem. Soc., Chem. Commun.*, 1983, 593–594.
12 K. Tanaka and F. Toda, *J. Chem. Soc., Perkin Trans. 1*, 1992, 943–944.
13 K. Tanaka and F. Toda, in *Organic Solid State Reactions*, ed. F. Toda, Kluwer Academic Publishers, Dordrecht, 2002, pp. 109–158.
14 K. Tanaka, F. Toda, E. Mochizuki, N. Yasui, Y. Kai, I. Miyahara and K. Hirotsu, *Angew. Chem., Int. Ed.*, 1999, **38**, 3523–3525.
15 F. Toda, in *Topics in Current Chemistry*, ed. E. Weber, Springer-Verlag, Berlin, 1988, vol. 149, pp. 211–238.
16 F. Toda, *Acc. Chem. Res.*, 1995, **28**, 480–486.
17 *Organic Solid-State Reactions*, F. Toda, ed., Kluwer Academic, Dordrecht, 2002.
18 K. Mori, O. Murai, S. Hashimoto and Y. Nakamura, *Tetrahedron Lett.*, 1996, **37**, 8523–8526.
19 L. R. MacGillivray, *J. Org. Chem.*, 2008, **73**, 3311–3317.
20 L. R. MacGillivray, G. S. Papaefstathiou, T. Friscic, T. D. Hamilton, D.-K. Bucar, Q. Chu, D. B. Varshney and I. G. Georgiev, *Acc. Chem. Res.*, 2008, **41**, 280–291.
21 L. R. MacGillivray, J. L. Reid and J. A. Ripmeester, *J. Am. Chem. Soc.*, 2000, **122**, 7817–7818.

22 X. Gao, T. Friscic and L. R. MacGillivray, *Angew. Chem., Int. Ed.*, 2004, **43**, 232–236.
23 D. B. Varshney, X. Gao, T. Friscic and L. R. MacGillivray, *Angew. Chem., Int. Ed.*, 2006, **45**, 646–650.
24 T. Bach, H. Bergmann and K. Harms, *Angew. Chem., Int. Ed.*, 2000, **39**, 2302–2304.
25 C. Müller, A. Bauer and T. Bach, *Angew. Chem., Int. Ed.*, 2009, **48**, 6640–6642.
26 A. Bauer, F. Westkamper, S. Grimme and T. Bach, *Nature*, 2005, **436**, 1139–1140.
27 C. Müller, A. Bauer, M. M. Maturi, M. C. Cuquerella, M. A. Miranda and T. Bach, *J. Am. Chem. Soc.*, 2011, **133**, 16689–16697.
28 J.-i. Mizoguchi, Y. Kawanami, T. Wada, K. Kodama, K. Anzai, T. Yanagi and Y. Inoue, *Org. Lett.*, 2006, **8**, 6051–6054.
29 D. F. Cauble, V. Lynch and M. J. Krische, *J. Org. Chem.*, 2003, **68**, 15–21.
30 L. Zhang and E. Meggers, *Acc. Chem. Res.*, 2017, **50**, 320–330.
31 K. L. Skubi, J. B. Kidd, H. Jung, I. A. Guzei, M.-H. Baik and T. P. Yoon, *J. Am. Chem. Soc.*, 2017, **139**, 17186–17192.
32 F. Pecho, Y.-Q. Zou, J. Gramüller, T. Mori, S. M. Huber, A. Bauer, R. M. Gschwind and T. Bach, *Chem. – Eur. J.*, 2020, **26**, 5190–5194.
33 N. Vallavoju, S. Selvakumar, S. Jockusch, M. P. Sibi and J. Sivaguru, *Angew. Chem., Int. Ed.*, 2014, **53**, 5604–5608.
34 N. Vallavoju, S. Selvakumar, S. Jockusch, M. T. Prabhakaran, M. P. Sibi and J. Sivaguru, *Adv. Synth. Catal.*, 2014, **356**, 2763–2768.
35 N. Vallavoju, S. Selvakumar, B. C. Pemberton, S. Jockusch, M. P. Sibi and J. Sivaguru, *Angew. Chem., Int. Ed.*, 2016, **55**, 5446–5451.
36 E. Kumarasamy, A. J.-L. Ayitou, N. Vallavoju, R. Raghunathan, A. Iyer, A. Clay, S. K. Kandappa and J. Sivaguru, *Acc. Chem. Res.*, 2016, **49**, 2713–2724.
37 R. Telmesani, S. H. Park, T. Lynch-Colameta and A. B. Beeler, *Angew. Chem., Int. Ed.*, 2015, **54**, 11521–11525.
38 F. Mayr, R. Brimioulle and T. Bach, *J. Org. Chem.*, 2016, **81**, 6965–6971.
39 E. M. Sherbrook, M. J. Genzink, B. Park, I. A. Guzei, M.-H. Baik and T. P. Yoon, *Nat. Commun.*, 2021, **12**, 5735.
40 E. M. Sherbrook, H. Jung, D. Cho, M.-H. Baik and T. P. Yoon, *Chem. Sci.*, 2020, **11**, 856–861.

